Observation of stochastic resonance in a liquid-crystal light valve with optical feedback induced by colored noise in the driving voltage

Yoshitomo Goto [1,2] Atsuya Shishibe,[1] Hiroshi Orihara [3] Stefania Residori,[4,5] and Tomoyuki Nagaya[1,6]

[1]*Graduate School of Engineering, Oita University, Oita 870-1192, Japan*
[2]*Beppu University Junior College, Beppu 874-8501, Japan*
[3]*Division of Applied Physics, Hokkaido University, Sapporo 060-8628, Japan*
[4]*Institut de Physique de Nice, Université de Nice Sophia-Antipolis, 06560 Valbonne, France*
[5]*HOASYS, 06560 Valbonne, France*
[6]*Division of Natural Sciences, Oita University, Oita 870-1192, Japan*

Stochastic resonance is a noise phenomenon that benefits applications such as pattern formation, neural systems, microelectromechanical systems, and image processing. This study experimentally clarifies that the orientation of the liquid crystal molecules was switched between two stable positions when stochastic resonance was induced by colored noises in a liquid crystal light valve with optical feedback. Ornstein-Uhlenbeck and dichotomous noises were used for colored noise, and the noise was applied to the drive voltage of the liquid crystal light valve. The signal-to-noise ratio was measured with respect to changes in the noise type, noise intensity, and autocorrelation time of the noise. It was found that typical stochastic resonance was observed with a noise autocorrelation time of approximately 20 ms or more for both noise types, and dichotomous noise further enhanced the stochastic resonance compared to the Ornstein-Uhlenbeck noise. This suggests that it is possible to maximize stochastic resonance in a liquid crystal light valve by optimizing the conditions of colored noise.

I. INTRODUCTION

Stochastic resonance (SR) is a widely known noise-induced phenomenon by which noise added to a weak signal can improve its detection in nonlinear dynamical systems [1,2]. In particular, the benefit of SR has been discussed intensively with regard to pattern formation [3,4], neural systems [5], microelectromechanical systems [6], and image processing [7–9].

In the field of optics, SR in a system with two-dimensional spread has attracted substantial attention from the perspective of applications such as image sensing. Recently, a new type of SR, based on modulation instability in a photorefractive medium has been proposed, and the results of reconstruction of noisy images have been reported [10–12].

One of the best-known optical elements for realizing a two-dimensional spreading optical system is a spatial light modulator (SLM) [13], an optically addressed (OASLM) or liquid crystal light valve (LCLV), composed of a liquid crystal (LC) and a photoconductor, for which the driving can be induced by the light impinging on the photosensitive side. In 1995, the first experimental study on SR in an LCLV system was performed by Sharpe *et al.* [14]. They used a ferroelectric-liquid-crystal (FLC) optically addressed SLM. As the director of LC molecules **n**, a unit vector in the direction of the local average orientation of the symmetry axes of the LC molecules can be switched between two stable positions on a smectic cone by an external electric field, the appearance of SR was expected. They successfully observed the typical SR

phenomenon in the LCLV by measuring the signal-to-noise ratio (SNR) of the optical output signal reflecting the response of the director. Although they observed a circular area with a diameter of 5 mm, the system could be regarded as one-dimensional because the switching of the director in the area was almost homogeneous, i.e., single-domain switching.

To date, several types of LCLVs have been developed. One of the most common types is the LCLV composed of nematic LCs. In contrast to a ferroelectric LCLV, the director of the LC in a nematic LCLV changes monotonically by the effective amplitude of the electric voltage above the Frederiks transition voltage. In other words, the director in a nematic LCLV is monostable under an electric voltage. To realize the bistability of the director angle, positive feedback is required on a nematic LCLV. This feedback can be implemented by configuring an optical feedback loop to the LCLV, which makes the system bistable through subcritical bifurcation [15–17].

An LCLV with optical feedback provides a two-dimensional bistable dynamical system and shows a large variety of spatiotemporal patterns; thus several researchers have shown an interest not only in the pattern dynamics [15–21] but also the SR [22] over the past few decades.

Sharpe *et al.* investigated SR in a two-dimensional array of bistable components generated in a nematic LCLV with optical feedback [22]. Their pioneering work was to apply spatially varying noise to a two-dimensional array of bistable regions constructed on the LCLV, but they observed a broad range of SNRs, which was an unusual property of SR because of the Gaussian intensity profile of the expanded incident laser

light. To date, typical SR has not been observed in an LCLV with optical feedback.

Thus, the main purpose of this study is to clarify the existence of typical SR in an LCLV with optical feedback. In addition, we focus on the color of noise because the enhancement of SR by colored noise has attracted significant attention in spatially extended systems [23,24]. In the research area of SR, there are two widely discussed types of colored noise: dichotomous (DM) noise and Ornstein-Uhlenbeck (OU) noise. Some theoretical and numerical studies have claimed that dichotomous noise enhances SR [25,26]. The same effect has been claimed for OU noise [6,27,28].

Corresponding to these theoretical studies, several experimental studies that support the theoretical results with DM or OU noise have been reported [6,29,30]. Although DM and OU noises have both attracted substantial interest in relation to the enhancement of SR, there has been little research on LCLVs with optical feedback. Sharpe *et al.* used light transmitted by a controlled liquid crystal display (LCD) to add noise to the light intensity so that the optical applied noise could exhibit spatial and temporal variations [22]. Using LCD-transmitted light, however, seems to result in coloring the noise owing to the LCD frame rate or LC response time, and the noise color was not adequately elucidated in the article. We consider that the typical SR phenomenon may be observable if we apply colored noise with a suitable correlation time to an LCLV system and observe the response of the LC molecules in a small single-domain area. To demonstrate the influence of the difference in time characteristics of DM and OU noises on the enhancement of SR, we excluded the effect of signal processing with two-dimensional spatial characteristics that is a feature of an LCLV and applied spatially uniform noise to the LCLV.

This paper is organized as follows: In Sec. II, we provide the details of the experimental setup. Then, in Sec. III, we describe the noise type and color employed in the experiment. We present the experimental results and discussion in Sec. IV. Finally, in Sec. V, we summarize our demonstration and findings.

II. EXPERIMENT

As shown in Fig. 1(a), an LCLV (Hamamatsu PAL-SLM) comprises three layers: a nematic LC layer, dielectric mirror layer, and photoconductive plate layer, sandwiched between indium tin oxide–(ITO) coated glass plates. Coating an aligning agent on the surface of the glass plate and the dielectric mirror face to the LC, the LC molecules are aligned parallel to the glass plates. An external alternating voltage is applied between the ITO electrodes, and the tilt angle of the director θ measured from a plane parallel to the glass plates is controlled by the amplitude of the voltage V and the intensity of writing light I_W that illuminates the photoconductive plate. For simplicity, we ignore the change in θ along the direction perpendicular to the glass plates. The tilt angle θ can be considered as averaged along with the LC thickness. In our LCLV, the thickness of the LC layer is $d = 9\,\mu$m. Light from the LC layer side (reading side) passes through the LC layer and is reflected by the dielectric mirror layer. Due to the dielectric anisotropy of the LC layer, this reading-side light has modified
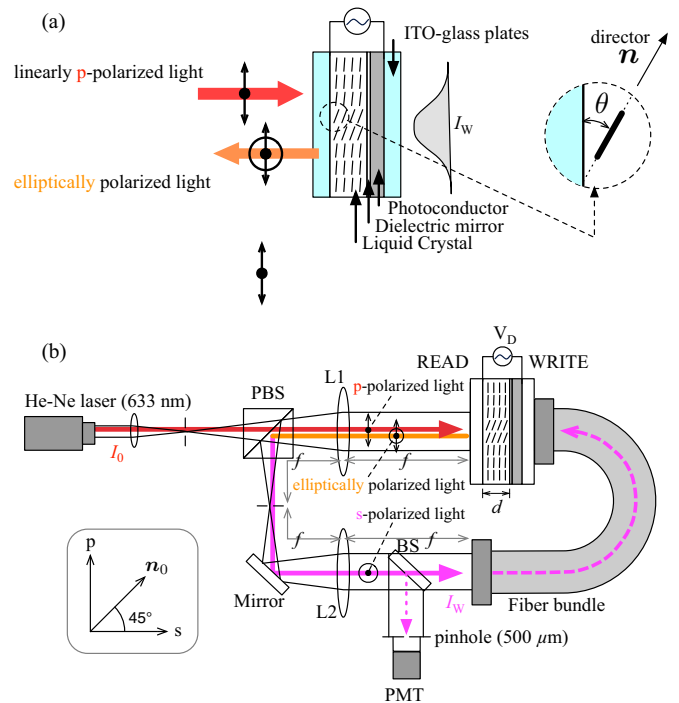

FIG. 1. Optical circuit to observe SR. (a) Structure of the LCLV and polarization characteristics of incoming and outgoing light. (b) Optical setup of the LCLV with feedback.

its phase and polarization. On the other side (writing side) of the LCLV, light illuminated onto an area of the photoconductive plate increases the voltage applied to the LC layer and causes LC reorientation, so that the amount of birefringence of the LC layer changes as $\Delta n \cong (n_e - n_o)\cos^2\theta$ [15], where n_e is the extraordinary index of refraction ($\parallel$ to $\boldsymbol{n}$) and n_o is the ordinary index of refraction ($\perp$ to $\boldsymbol{n}$) of the LC, in the area corresponding to the intensity of the writing-side light.

As θ depends on V and I_W, there are two general methods of adding noise to the LCLV: The first is to add an electrical noise signal to the magnitude of the LCLV's driving voltage, and the second is to add optical noise to the intensity of the light on the photoconductor layer [22]. From the perspective of the relation between SR and noise, the former method has various advantages, such as good controllability of the properties of noise type, strength, and color. Despite these advantages, there has been no study concerning SR in an LCLV with optical feedback by applying noise to the LCLV's driving voltage. Thus, we designed this experiment to experimentally demonstrate SR in an LCLV with optical feedback and with noise applied to the LCLV's driving voltage.

In contrast to the Sharpe *et al.* method of adding spatially variant noise to light [22], we did not consider spatial variations and applied spatially uniform noise to the LCLV driving voltage. This approach enabled us to control the noise type and color precisely.

The optical circuit to observe the SR is shown in Fig. 1(b). A horizontally polarized laser beam (633 nm) emitted from a He-Ne laser (NEOARC MS-30) was expanded by a spatial filter and injected into the LC layer of the LCLV. To utilize the maximum birefringence of the LC, the optical axis of

the LCLV under no applied voltage, n_0, was set to $45°$ from the horizontal plane. The laser beam was reflected by the dielectric mirror in the LCLV and fed back to the writing side by lenses and a coherent optical fiber bundle. The focal length of both lenses was 250 mm.

When the writing side was locally illuminated, photocarriers were correspondingly nucleated in the photoconductor layer. Consequently, in the reading-side area facing the illuminated area, the effective electric voltage V_{eff} applied across the LC layer increased and reoriented the LC molecules. Thus, the feedback was established between the LC reorientation and local electric field.

The feedback loop is closed by the optical fiber bundle attached to the rear and photosensitive side of the LCLV. It coherently transfers the optical field at the image plane of the lens L2 onto the photoconductor of the LCLV. Thus, the outgoing light from a point at the reading-side of LCLV is simply fed back to a back of the same point at the writing-side of LCLV. The feedback light intensity $I_W(t)$, which reflects the tilt angle of the director in the LCLV, was measured using a beam sampler (BS) and a photomultiplier (PMT, Hamamatsu H5783-01). A photocurrent emitted from the PMT was converted into voltage V_{PMT} by a charge amplifier (Hamamatsu C7319). The time evolution of V_{PMT} was recorded by a digital acquisition board (National Instruments PCIe-6361). Owing to the Gaussian profile of the expanded laser beam, the spatial distribution of the director was slightly inhomogeneous in the center area of the LCLV by about 1 cm in diameter. To ignore the effects of the inhomogeneous distribution and to prepare an ideal bistable system that can be regarded as homogeneous, we limited the measurement area to a local microregion using a pinhole of diameter $500\,\mu\text{m}$ located at the center of the sampled beam and we measured the light intensity passing through the pinhole.

Owing to the birefringence of the LC, the outgoing light from the reading side of the LCLV was elliptically polarized. The phase shift between the ordinary and extraordinary rays, ϕ, i.e., the retardation, is expressed as

$$\phi = 4\pi \frac{[n_{\text{eff}}(\theta) - n_o]d}{\lambda}, \tag{1}$$

where λ is the wavelength of the laser beam, d is the thickness of the LC layer, and $n_{\text{eff}}(\theta)$ is the effective refractive index for the extraordinary ray when the director is tilted from the glass plates by angle θ and is expressed as

$$n_{\text{eff}}(\theta) = \frac{n_o n_e}{\sqrt{n_o^2 \cos^2\theta + n_e^2 \sin^2\theta}}. \tag{2}$$

As θ depends on the effective voltage V_{eff} at the position of the incident beam, the phase shift ϕ also depends on V_{eff}. The tilt angle θ monotonically increases as the voltage rises and converges to $90°$. However, its convergence toward $90°$ is very slow because an infinite voltage strength is required to align the director perpendicular to the glass plates. As a result, $n_{\text{eff}}(\theta)$ decreased slowly from n_e to n_o and ϕ from $4\pi d(n_e - n_o)/\lambda$ to 0, as V_{eff} increased.

As a polarizing beam splitter (PBS) reflects only the vertical component of the elliptically polarized light, the intensity

of the writing light I_W can be expressed as

$$I_W = \frac{I_0 e^{-\gamma}(1 - \cos\phi)}{2}, \tag{3}$$

where I_0 is the intensity of the incident beam and γ is the effective optical loss representing the absorption in the optical circuit.

The frequency of the voltage applied to the LCLV was fixed at $f_0 = 1\,\text{kHz}$. The amplitude of the voltage was modulated by the weak sinusoidal signal V_s ($f_s = 1\,\text{Hz}$) with noise ξ. Hence, the modulated voltage applied to the LCLV V_D can be expressed as

$$V_D = \{V_s(t) + \xi(t) + V_0\}\sin(2\pi f_0 t), \tag{4}$$

where $\xi(t)$ is a zero mean, DM noise, or OU noise, and V_0 is the amplitude of the applied voltage without modulation. Each signal was supplied by arbitrary waveform generators (NF WF-1944, WF-1946B). For the multiplier, an AD633 chip was used for the amplitude modulation of V_D.

III. NOISE

Both the DM and OU noises used in this experiment have an exponential autocorrelation function. Concerning both their waveforms and the distribution function of their noise value, however, there are intrinsic differences. DM noise, or random telegraph noise, $\xi^{\text{DM}}(t)$ is a random variable that transits between two states $A_\pm$ randomly in time [31,32]. The transition rate from A_+ to A_- is k_+, and k_- from A_- to A_+. This two-step process can be described by the following master equation:

$$\frac{d}{dt}\begin{bmatrix} P(A_+, t|x, t') \\ P(A_-, t|x, t') \end{bmatrix} = \begin{pmatrix} -k_+ & k_- \\ k_+ & -k_- \end{pmatrix}\begin{bmatrix} P(A_+, t|x, t') \\ P(A_-, t|x, t') \end{bmatrix}, \tag{5}$$

where $P(A_+, t|x, t')$ is the conditional probability that $\xi^{\text{DM}}(t)$ will assume the value A_+ under the condition $\xi(t') = x$ ($t' < t$). In this study, we consider a symmetrical DM noise, for which $A_+ = -A_- \equiv A$ and $k_+ = k_- \equiv k$. Using this simplification, the mean and normalized autocorrelation function of the DM noise are expressed as

$$\langle \xi^{\text{DM}}(t) \rangle = 0, \tag{6}$$

$$\langle \xi^{\text{DM}}(t_0)\xi^{\text{DM}}(t) \rangle / \langle \xi^{\text{DM}}(t_0)^2 \rangle = \exp\left(-\frac{|t - t_0|}{\tau_{\text{DM}}}\right), \tag{7}$$

respectively, where τ_{DM} is the characteristic correlation time of the DM noise.

The OU noise $\xi^{\text{OU}}(t)$ is governed by the stochastic differential equation

$$\frac{d\xi^{\text{OU}}(t)}{dt} = \frac{1}{\tau_{\text{OU}}}\xi^{\text{OU}}(t) + D\xi^{\text{GWN}}(t), \tag{8}$$

where τ_{OU} is the correlation time of the OU noise, $\xi^{\text{GWN}}(t)$ is the Gaussian white noise, and D is the strength constant of the Gaussian white noise [25,31]. As with the DM noise, the OU noise is also characterized by $\langle \xi^{\text{OU}}(t) \rangle = 0$ and $\langle \xi^{\text{OU}}(t_0)\xi^{\text{OU}}(t) \rangle / \langle \xi^{\text{OU}}(t_0)^2 \rangle = \exp(-|t - t_0|/\tau_{\text{OU}})$.
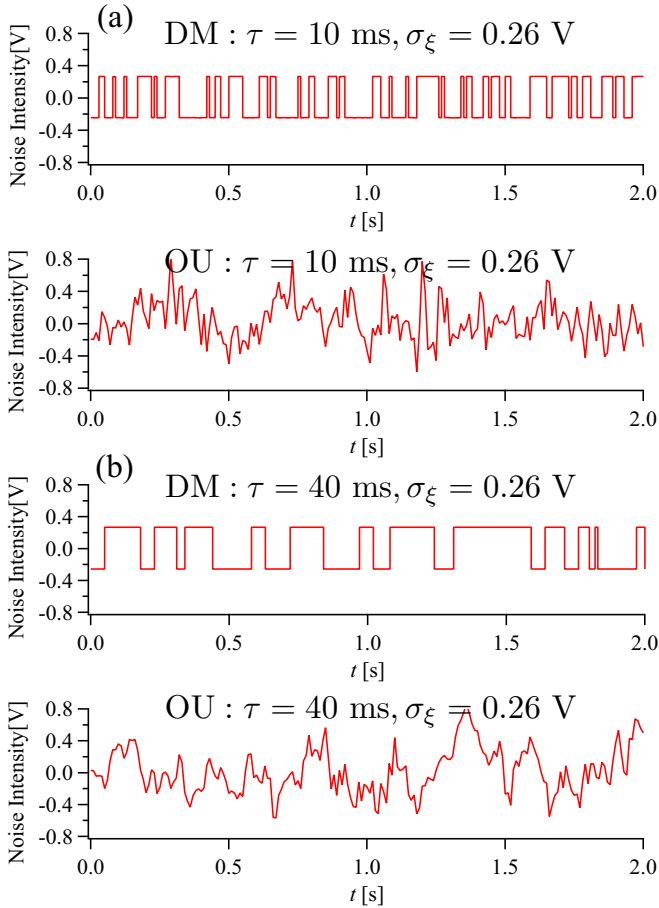
FIG. 2. Time series of DM and OU noises for two different correlation times, τ, and the same noise strength, σ_ξ. (a) $\tau = 10$ ms, $\sigma_\xi = 0.26$ V; (b) $\tau = 40$ ms, $\sigma_\xi = 0.26$ V.

The DM [33] and OU [34] noises are generated numerically and stored in the memories of the arbitrary waveform generator (ARB) and supplied by the ARB. Figure 2 presents two typical time-series plots for DM and OU noise with different autocorrelation times and the same noise strength σ_ξ. The autocorrelation function of the DM and OU noise with $\tau = 10$ ms is shown in Fig. 3. The curves are identical if their autocorrelation times are the same value.
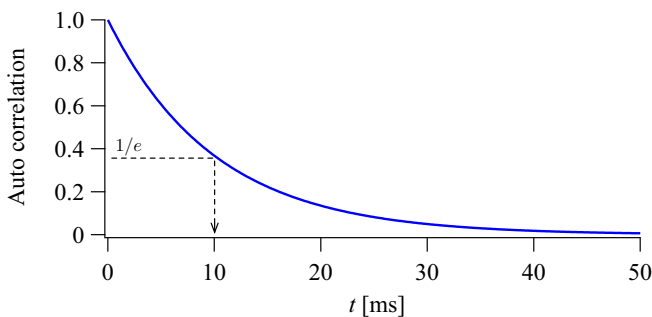

FIG. 3. Autocorrelation of DM and OU noises ($\tau = 10$ ms), defined as $\langle \xi(t_0)\xi(t) \rangle / \langle \xi(t_0)^2 \rangle$. Both sets of data fall on an identical curve.
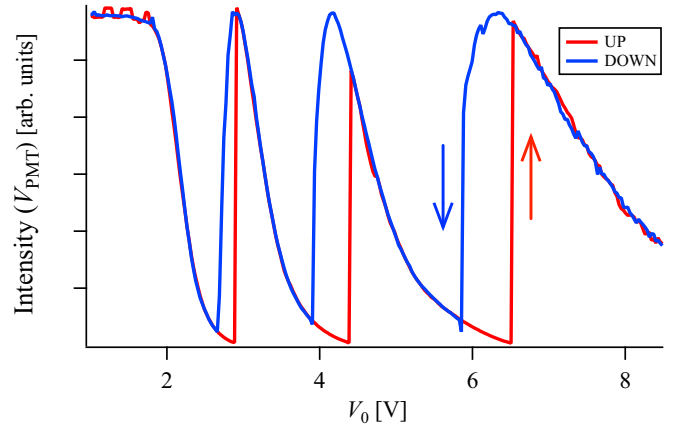

FIG. 4. V_0-V_{PMT} curves and hysteresis loops.

IV. RESULTS AND DISCUSSION

As mentioned above, the tilt angle of the director θ determines the phase shift ϕ between the ordinary and extraordinary rays of outgoing light from the reading side of the LCLV, and ϕ provides feedback to θ. This situation causes the time-dependent dynamics of $\phi(t)$. The phenomenological model of these dynamics $\phi(t)$ has been proposed and confirmed through experiments [16,17]. As we are observing a small area at the center of the LCLV, we can ignore the spatial dependence of ϕ. The equation of motion for ϕ is then expressed as

$$\tau_{\mathrm{LC}} \frac{\partial}{\partial t} \phi(t) = -\phi(t) + p - p \frac{s(V_0)a(V_0)I_W(\phi) + b(V_0)}{a(V_0)I_W(\phi) + 1}, \quad (9)$$

where τ_{LC} and p are constants characterizing the temporal relaxation of ϕ and maximum phase shift, respectively, and s, a, and b are constants that depend on the voltage applied to the LCLV. In equilibrium, ϕ shows bistability for V_0 in some regions. Consequently, I_W shows bistability in the V_0-I_W curve. In this experiment, the PMT is employed to evaluate I_W such that the bistability is observed in the V_0-V_{PMT} curve, where V_{PMT} is the output signal of the PMT that reflects the intensity of I_W.

Figure 4 shows the V_0-V_{PMT} curves for $I_0 = 0.18$ mW/cm^2 obtained experimentally. There are three hysteresis loops, with respect to increasing and decreasing V_0, in which the director has bistability. In this study, we observed the SR in the second bistable region near 4 V.

Figure 5 shows a schematic diagram of the relations between the width of the bistable region around $V_0 = 4.2$ V, signal strength V_s, and noise strength σ_ξ. The sinusoidal signal strength V_s, which modulates the amplitude of the AC voltage of 1 kHz, was sufficiently small relative to the width of the bistable region V_{width} such that the transitions between the high and low V_{PMT} states would not occur in the absence of noise. The values of θ for the high and low states at $V_0 = 4.16$ V (blue broken line) are 46.8° and 53.2°, respectively. To induce the transition, the noise strength σ_ξ was gradually increased. The total strength of the sinusoidal signal and the noise $|V_s + \sigma_\xi|$ acts as the effective strength of modulation for V_D; in the case of $|V_s + \sigma_\xi| > V_{\mathrm{width}}$, the transition can be expected to be enhanced. Hereafter, we set $V_0 = 4.16$ V.
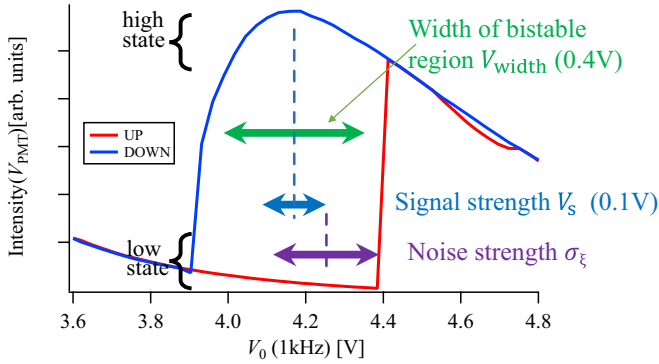
FIG. 5. Relations between width of the bistable region, signal strength, and noise strength. The values of θ in the high and low states can be estimated to be about $46.8°$ and $53.2°$, respectively.

Figure 6 illustrates the typical time series of V_{PMT}, a signal of 1 Hz sinusoidal modulation, and a noise. When σ_ξ is not strong enough, as shown in V_{PMT} with $\sigma_\xi = 0.24$ V in Fig. 6, V_{PMT} remained at the high state and no transition occurred. However, when $\sigma_\xi > 0.3$ V, as shown in V_{PMT} with $\sigma_\xi = 0.38$ V in Fig. 6, high-low transitions occurred occasionally, and it is easily recognized that the transition was stochastically synchronized with V_s. As σ_ξ increases further, the transition occurs randomly (not plotted). This phenomenon, in which the response of a system is enhanced as the noise strength increases at an optimal value, is typical of SR in a bistable system.

To discuss the SR phenomenon quantitatively, first we binarized $V_{PMT}(t)$ as $B_{PMT}(t)$ by a suitable threshold voltage, as with Sharpe *et al.* [22], and plotted it in the middle of Fig. 7 to distinguish the high and low states more clearly. We then introduced an SNR defined as

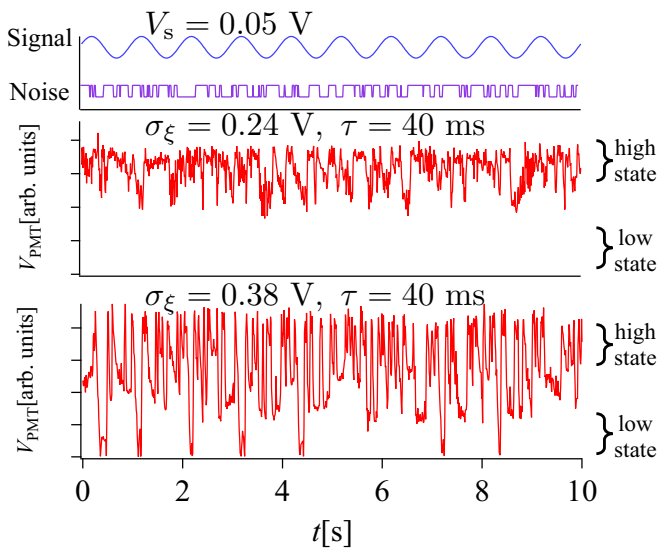$$\text{SNR} = 10 \log_{10} \frac{Ps_{\text{peak}}}{Ps_{\text{back}}}, \qquad (10)$$

FIG. 6. Time series of the sinusoidal modulation signal, DM noise of $\tau = 40$ ms, and V_{PMT}, which show high-low transitions induced by sufficient strength of the noise ($\sigma_\xi = 0.38$ V).
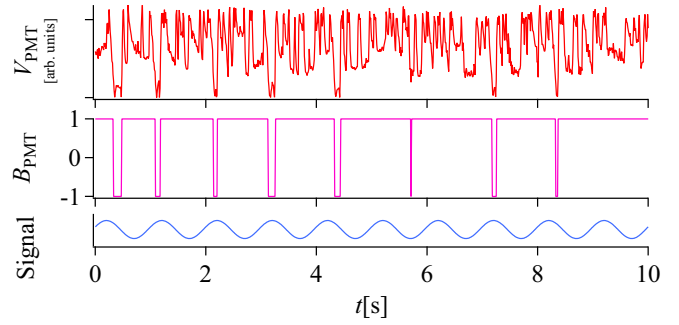

FIG. 7. $V_{PMT}(t)$, $B_{PMT}(t)$, and the sinusoidal signal. We replotted $V_{PMT}(t)$ using the same data as in Fig. 6. $B_{PMT}(t)$ was calculated by binarizing $V_{PMT}(t)$ with a threshold of 2.0 V in this figure.

where Ps_{peak} and Ps_{back} are the maximum of the power spectral density of $B_{PMT}(t)$ measured at the frequency of V_s ($= 1.0$ Hz) and the amplitude of the broadband noise background measured around the frequency of V_s, respectively; they can be obtained from the power spectral density plot (Fig. 8).

In Fig. 9, we plot SNR versus σ_ξ for different values of τ of the DM and OU noises. The SNR dependence on noise intensity shows that the SNR increases with increasing noise intensity and then decreases in the cases of both DM and OU noises, which is the characteristic behavior of SR. In comparison with Figs. 9(a) and 9(b), DM noise is superior to OU noise for enhancing SR in $\tau \geqslant 20$ ms. This phenomenon, in which the SR is enhanced by the DM noise, agrees with the studies suggesting that colored non-Gaussian noise enhances SR [26,35,36].

Regarding the noise correlation time dependence of the SNR, shown in Fig. 9, when $\tau \leqslant 10$ ms, the SNR is small, and when $\tau = 5$ ms, no resonance is observed even when the noise intensity is increased, which is not an effect of the cut-off frequency ($1/f_0 \sim 1$ ms). Hence, the SNR at $\tau = 5$ ms is not plotted. Furthermore, we could not observe any significant statistical value of resonance with Gaussian white noise, which is not plotted in Fig. 9 either. As DM and OU noises are known to reduce to Gaussian white noise in the limit of $\tau \to 0$ [32,37], it can be understood that these no-resonances are both due to a sufficiently small τ. This suppression of SR
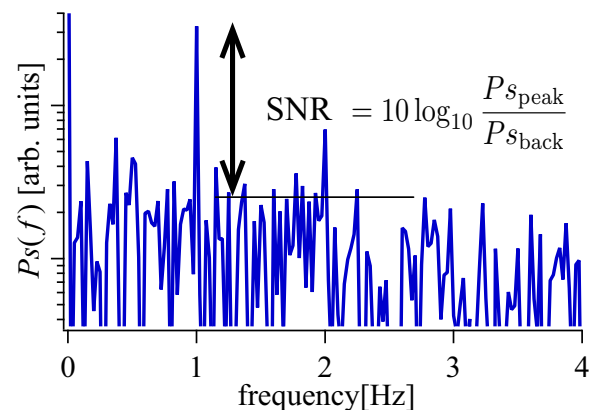

FIG. 8. Power spectrum density plot and SNR definition (plot for DM noise of $\tau = 50$ ms and $\sigma_\xi = 0.36$ V).
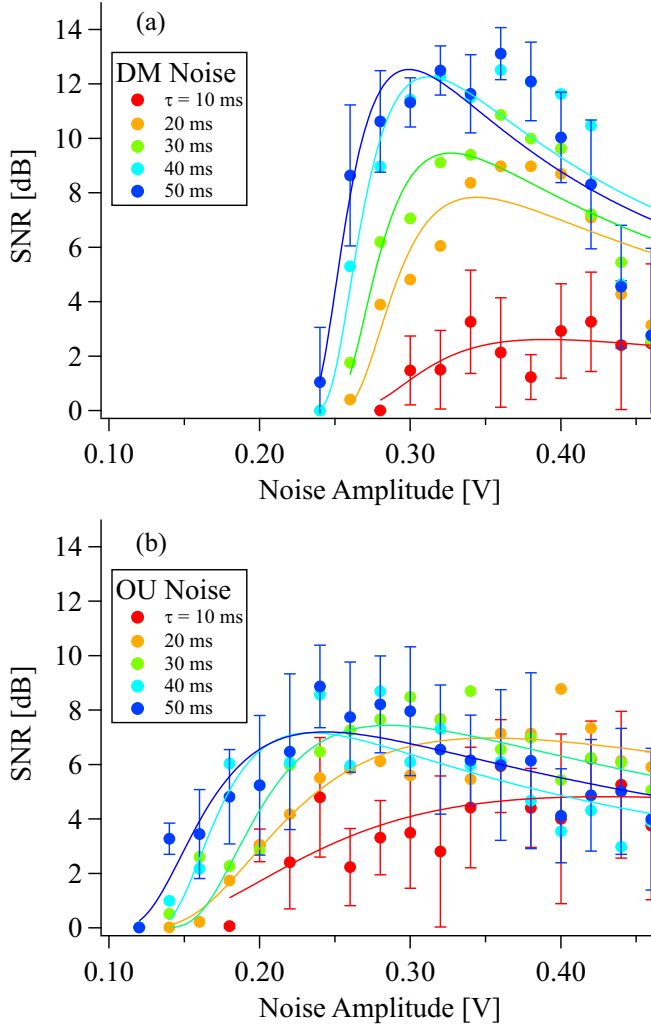
FIG. 9. Resonance curves from (a) DM and (b) OU noises for different values of τ. Error bars are omitted for clarity in cases of $\tau = 20$–40 ms. Each circle point is the mean value of 10 measurements of SNRs, which are calculated from the time series of 80 s $V_{PMT}(t)$. The error bars show the standard error SNRs in each condition.

by white noise has been reported in a linear system driven by multiplicative noise [38–40]. In this respect, we believe that the experimental system in this study was driven by multiplicative noise for the following reasons. Considering the ϕ dependence of the I_W in Eq. (3), the third term of Eq. (9) is a strongly nonlinear function of V and ϕ, and the nonlinearity has been recognized by many previous studies experimentally [15,16,41]. When we applied the noise to the voltage V, the effect of the noise by the third term depends on the state V and ϕ of the system, and its dependence on ϕ makes it a multiplicative noise. Thus, the no-resonances agree with Refs. [38–40] as far as the system could be regarded as an approximately linear system. However, we did not evaluate the linearity under experimental conditions because it was not the main purpose of this study.

As τ gradually increases from 10 ms, the noise becomes more colored and the SNR increases. The SR abruptly appears strongly at $\tau = 20$ ms or higher, and then at $\tau = 40$ ms or higher, the change is saturated. However, this phenomenon, by which SR is enhanced with an increase in τ, does not agree with some prior studies, such as the theoretical results of Fuentes *et al.* [35], or the experimental results of Dunn *et al.* [6] and Misono *et al.* [30], in which SR decreased with an increase in τ. One reason for this disparity may be the response time of the change in the tilt angle of the director in the LCLV to the external force. The response time of the director in the present system was experimentally estimated to be approximately 15–50 ms. Consequently, in the case in which τ is smaller than the lower limit of the LCLV response time, it is considered that the colored noise cannot contribute as an external force that causes a change in the tilt angle of the director. Das *et al.* [42] reported that the two-state system response is maximized theoretically and numerically when the internal timescale of the system and the DM noise correlation time are close, which is consistent with our results.

To discuss the effect of the response time of the director in the LCLV to external force and the correlation time of noise on the appearance of SR based on the framework of Das *et al.* [42], we have to evaluate the response time and potential shape of the LCLV precisely, and it is necessary to consider how they are affected by noise, which is not the main purpose of this study. In future work, we will evaluate the correspondence between the theoretical results and our experimental results.

Sharpe *et al.* [22] observed SR despite applying Gaussian white noise in their previous research on LCLVs, but in their experiments, Gaussian white noise was applied to the LCD to generate optical noise. Therefore, the optical noise applied to the LCLV should have been the colored noise reflecting the response time of the LCD, as we mentioned above. Considering this, their results agree with our results for SR observed in colored noise. If we find this agreement, it is expected that the SR in a two-dimensional array, achieved by Sharpe *et al.*, can be further enhanced by optimizing the noise conditions. Indeed, we expect that the definition of optimal noise conditions by the electrical driving voltage could be used in future works for spatial SR with optical addressing.

V. CONCLUSION

We clarified the appearance of SR using colored noise in the driving voltage of an LCLV with an optical feedback system. We also showed that DM noise is superior to OU noise for enhancing SR. Furthermore, it was clearly shown that the SNR at SR exhibits a noise autocorrelation time dependency. These results could be discussed in relation to the autocorrelation time of colored noise and the response time of LC molecules inside the LCLV.

In the future, if these can be further understood theoretically and experimentally, the phenomenon of two-dimensional SR in an LCLV can be sensitized, and the possibilities for application can be increased.

[1] S. Fauve and F. Heslot, Phys. Lett. A **97**, 5 (1983).

[2] K. Wiesenfeld and F. Moss, Nature **373**, 33 (1995).

[3] H. Zhonghuai, Y. Lingfa, X. Zuo, and X. Houwen, Phys. Rev. Lett. **81**, 2854 (1998).

[4] S. Scarsoglio, P. D'Odorico, F. Laio, and L. Ridolfi, Ecol. Complex. **10**, 93 (2012).

[5] D. Guo, M. Perc, Y. Zhang, P. Xu, and D. Yao, Phys. Rev. E **96**, 022415 (2017).

[6] T. Dunn, D. N. Guerra, and P. Mohanty, Eur. Phys. J. B **69**, 5 (2009).

[7] R. K. Jha and R. Chouhan, Sign. Image Video Process. **8**, 339 (2012).

[8] R. Peng, H. Chen, P. K. Varshney, and J. H. Michels, *Proceedings of the 2007 IEEE/NIH Life Science Systems and Applications Workshop*, 253 (IEEE, Los Alamitos, CA, 2007).

[9] R. Chouhan, R. K. Jha, and P. K. Biswas, IET Image Process. **7**, 174 (2013).

[10] X. Feng, H. Liu, N. Huang, Z. Wang, and Y. Zhang, Sci. Rep. **9**, 3976 (2019).

[11] J. Han, H. Liu, N. Huang, Z. Wang, Y. Zhang, and J. Chi, Appl. Phys. Express **12**, 012007 (2019).

[12] D. V. Dylov and J. W. Fleischer, Nat. Photon. **4**, 323 (2010).

[13] In this paper, we use OASLM as having the same meaning as LCLV.

[14] J. P. Sharpe, N. Sungar, and N. Macaria, Opt. Commun. **114**, 25 (1995).

[15] S. Residori, Phys. Rep. **416**, 201 (2005).

[16] T. Nagaya, T. Yamamoto, T. Asahara, S. Nara, and S. Residori, J. Opt. Soc. Am. B **25**, 74 (2008).

[17] Y. Iino and P. Davis, J. Appl. Phys. **87**, 8251 (2000).

[18] S. Residori, A. Petrossian, T. Nagaya, C. S. Riera, and M. G. Clerc, Phys. D **199**, 149 (2004).

[19] T. Nagaya, S. Nara, and S. Residori, Phys. D **238**, 2078 (2009).

[20] T. Nagaya, S. Nara, and S. Residori, Mol. Cryst. Liq. Cryst. **511**, 25/[1495] (2009).

[21] R. Neubecker, G.-L. Oppo, B. Thuering, and T. Tschudi, Phys. Rev. A **52**, 791 (1995).

[22] J. P. Sharpe, N. Sungar, M. Swaney, K. Carrigan, and S. Wheeler, Phys. Rev. E **67**, 056222 (2003).

[23] Y. Li, B. Jia, X. Zhang, and Y. Yang, Eur. Phys. J.: Spec. Top. **227**, 821 (2018).

[24] H.-G. Gu, B. Jia, Y.-Y. Li, and G.-R. Chen, Phys. A **392**, 1361 (2013).

[25] P. Hänggi, P. Jung, C. Zerbe, and F. Moss, J. Stat. Phys. **70**, 25 (1993).

[26] R. Rozenfeld, A. Neiman, and L. Schimansky-Geier, Phys. Rev. E **62**, R3031 (2000).

[27] L. Gammaitoni, P. Hänggi, P. Jung, and F. Marchesoni, Rev. Mod. Phys. **70**, 223 (1998).

[28] S. Zhong and H. Xin, Chem. Phys. Lett. **333**, 133 (2001).

[29] R. N. Mantegna and B. Spagnolo, Il Nuovo Cimento D **17**, 873 (1995).

[30] M. Misono, T. Kohmoto, Y. Fukuda, and M. Kunitomo, Opt. Commun. **152**, 255 (1998).

[31] W. Horsthemke and R. Lefever, *Noise-Induced Transitions: Theory and Applications in Physics, Chemistry, and Biology*, Springer Series in Synergetics (Springer, Berlin, 2006).

[32] I. Bena, Int. J. Mod. Phys. B **20**, 2825 (2006).

[33] D. Barik, P. K. Ghosh, and D. S. Ray, J. Stat. Mech. (2006) P03010.

[34] D. T. Gillespie, Phys. Rev. E **54**, 2084 (1996).

[35] M. A. Fuentes, R. Toral, and H. S. Wio, Physica A **295**, 114 (2001).

[36] F. J. Castro, M. N. Kuperman, M. Fuentes, and H. S. Wio, Phys. Rev. E **64**, 051105 (2001).

[37] C. V. D. Broeck, J. Stat. Phys. **31**, 467 (1983).

[38] V. Berdichevsky and M. Gitterman, Europhys. Lett. **36**, 161 (1996).

[39] J.-H. Li and Y.-X. Han, Phys. Rev. E **74**, 051115 (2006).

[40] A. V. Barzykin and K. Seki, Europhys. Lett. **40**, 117 (1997).

[41] Y. Iino and P. Davis, J. Appl. Phys. **85**, 3399 (1999).

[42] D. Das and D. S. Ray, Phys. Rev. E **87**, 062924 (2013).